Quasi-Classical Trajectory Calculations of the Hydrogen Abstraction Reaction H + NH3

ARTICLE *in* THE JOURNAL OF PHYSICAL CHEMISTRY A · JUNE 2010

Impact Factor: 2.69 · DOI: 10.1021/jp101607n · Source: PubMed

2 AUTHORS:

Joaquin Espinosa-Garcia
Universidad de Extremadura
141 PUBLICATIONS **2,186** CITATIONS
SEE PROFILE

Jose C Corchado
Universidad de Extremadura
118 PUBLICATIONS **3,296** CITATIONS
SEE PROFILE

Quasi-Classical Trajectory Calculations of the Hydrogen Abstraction Reaction H + NH_3

Joaquín Espinosa-García* and José C. Corchado

Departamento de Química Física, Universidad de Extremadura, 06006 Badajoz (Spain)

Received: February 23, 2010; Revised Manuscript Received: May 4, 2010

On a new potential energy surface (PES-2009) recently developed by our group describing the H + NH_3 hydrogen abstraction reaction, we perform an exhaustive state-to-state dynamics study using quasi-classical trajectory (QCT) calculations at collision energies between 15 and 50 kcal mol^{-1}. The reaction cross section is very small, corresponding to a large barrier height and reproducing other theoretical measurements. Most of the available energy appears as product translational energy (∼50%) with the H_2 diatomic product being vibrationally cold ($v' = 0, 1$). The vibrational distribution of the triatomic NH_2 product shows that it is mostly found in its vibrational ground state (∼80%), with a small vibrational excitation in the bending mode (∼12%). This distribution varies little with the collision energy. The product angular distribution shows sideways−backward behavior at low energies, shifting the scattering toward the sideways hemisphere when the energy increases. The effect of the zero-point energy constraint on these dynamical properties was analyzed.

1. Introduction

The gas-phase H + NH_3 → H_2 + NH_2 hydrogen abstraction reaction plays an important role in the chemistry of ammonia. It is found to be extremely slow at low temperatures, although at high temperatures it plays a significant role in ammonia pyrolisis and combustion.

Kinetically, this reaction has been widely studied using various experimental techniques[1−6] and theoretical methods.[7−17] The extensive literature on the kinetics of this reaction contrasts with the paucity of dynamics studies. To the best of our knowledge, no experimental studies have been reported on this reaction, and only recently have six theoretical studies been reported.[12−17] Their focus has, however, been practically entirely on the reaction cross section, either per se or as a way to obtain the rate coefficients. The lack of experimental dynamics studies could be because state-to-state measurements are difficult to perform at low energies given that the H atoms, which are produced in a photolysis process, are hot. This situation is similar to the isoelectronic H + CH_4 hydrogen abstraction reaction, where the first measurement of the reaction cross section was reported by Valentini et al.[18] at 34.5 kcal mol^{-1} in 1992, and it was not until 2003 that Zare et al.[19] carried out the first measurements of the product angular distribution at 45 kcal mol^{-1}. In the title reaction, the situation is even worse because the barrier to reaction is even higher than that of the H + CH_4 reaction.

As was remarked above, the theoretical dynamics studies[12−17] have focused on the reaction cross section. Li et al.[13] and Zhang et al.[14] performed reduced dimensionality quantum mechanical (QM) dynamics studies using the semirigid vibrating rotor target (SVRT) model, whereas Yang and Corchado[15−17] performed QM dynamics studies using the time-dependent wave packet (TDWP) method. As is well known, the bottleneck in these dynamics studies is the construction of the potential energy surface (PES) describing the reactive system. The enormous effort needed in this process is responsible for the reduced number of surfaces that exist for this polyatomic reaction. In 1997, our group[11] reported the first analytical surface for this reaction, PES-1997, which was fitted to a combination of experimental and theoretical information; that is, it was semiempirical in nature. In 2005, Moyano and Collins[12] reported an interpolated potential surface for the title reaction based on a set of data points calculated at high ab initio level. The PES-1997 (with or without modifications) was used by several groups[13−17] to perform the aforementioned quantum dynamics calculations. However, recently, Yang and Corchado[15] observed a major drawback of the PES-1997, namely, that it describes incorrectly the NH_3 inversion motion, predicting incorrectly that the planar ammonia (D_{3h} symmetry) is ∼9 kcal mol^{-1} more stable than the pyramidal structure (C_{3v} symmetry). To correct this incorrect behavior of the NH_3 inversion and the other main deficiencies of the earlier PES-1997, together with its semiempirical character, we have recently reported[20] the construction of a new analytical potential energy surface, named PES-2009, which is a fit to very high level ab initio calculations.

An extensive kinetics study using variational transition state theory with semiclassical transmission coefficients over a wide temperature range, 200−2000 K, was described in that paper.[20] We found that the polyatomic PES-2009 surface reproduces a wide spectrum of experimental kinetics measurements, such as the forward and reverse rate coefficients, kinetic isotope effects, and so on, lending strong support to its applicability. In the present study, we go deeper into the understanding of the title reaction by studying its dynamics using quasi-classical trajectory (QCT) calculations based on the new PES. The article is structured as follows. Section II briefly outlines the PES and the computational details. The QCT results are presented in Section III and compared with the scarce theoretical information available. Finally, Section IV presents the conclusions.

II. Potential Energy Surface and Computational Details

Recently, our group constructed[20] an analytical PES describing the hydrogen abstraction channel of the polyatomic gas-phase H + NH_3 reaction. This surface, named PES-2009, is symmetric with respect to the permutation of the three equivalent hydrogen atoms, a feature that is especially interesting for dynamics calculations, and solves the main drawbacks of our earlier PES-1997. The development of the new functional form

* Corresponding author. E-mail: joaquin@unex.es.

10.1021/jp101607n
Published on Web 05/12/2010

was described in that work and therefore will be not repeated here. Basically, it consists of three LEP-type (London−Eyring−Polanyi) stretching terms (str), augmented by valence (val) bending terms. As input data in the calibration process, we used exclusively very high level ab initio calculations at the CCSD(T)/cc-pVTZ level.

QCT calculations[21−23] were carried out using the VENUS96 code,[24] customized to incorporate our analytical PESs. The accuracy of the trajectories was checked by the conservation of total energy and total angular momentum. The integration step was 0.01 fs, with an initial separation between the H atom and the ammonia center of mass of 6.0 Å. The vibrational and rotational energies were obtained by thermal sampling at 300 K. Experimentally, state-to-state dynamics studies are difficult to perform at low energies (0−10 kcal mol^{-1}) for the title reaction because the H atoms, which are produced in a photolysis process, are hot. Therefore, the reactant collision energies considered in the present work range from 15.0 to 50.0 kcal mol^{-1}, with intervals of 5.0 kcal mol^{-1}.

For each energy (15, 20, 25, 30, 35, 40, 45, and 50 kcal mol^{-1}), the maximum value of the impact parameter, b_{max}, was determined by calculating batches of 10 000 trajectories at fixed values of the impact parameter, b, systematically increasing the value of b until no reactive trajectories were obtained. The b_{max} value is 2.1 Å for all energies. The reaction probability, N_r/N_T, is the ratio of the number of reactive trajectories and the total number of trajectories, whereas the reaction cross section is defined as

$$\sigma_r = \pi b_{max}^2 (N_r/N_T) \tag{1}$$

Second, to compare with other theoretical QCT results, batches of 200 000 trajectories were calculated for each collision energy considered in this work (a total of 8 energies and 1 600 000 trajectories), where the impact parameter, b, was sampled from

$$b = b_{max} R^{1/2} \tag{2}$$

where R is a random number in the interval [0,1].

After each reactive trajectory, the final coordinates and momenta are used to calculate vibrational and rotational actions, which are rounded to the lowest integer (in units of $\hbar$) to obtain the quantum states of the products. Recently, our group[25] developed a semiclassical method to obtain vibrational action variables in polyatomic systems, named NMA (normal-mode analysis), with two versions, harmonic (NMA-HARM) and anharmonic (NMA-ANHARM). We checked the validity of this method by comparing it with the Einstein−Brillouin−Keller (EBK) semiclassical quantization of the action integral[26] for diatomic species, and to the fast Fourier transform (FFT) approach of Eaker and Schatz[27] for triatomic species using the ACTION computer code of Schatz.[28] In both cases, diatomic and triatomic species, which are the only cases where comparison is possible, both versions of the NMA method reproduce the results of these methods, with the main advantage being that the NMA approach is general for any polyatomic species.[25] This approach has been extensively described in a previous paper[25] and therefore will not be repeated in detail here. In brief, however, in NMA, we use as input the last geometry (coordinates and momenta) of the reactive trajectories. The projection of the displacement and momentum matrices onto the respective normal-mode space allows us to compute the kinetic and potential energies, and therefore the total vibrational energy, for each normal mode, i

$$(E_k)_i = \frac{1}{2\mu}(P_R)_i^2 \tag{3}$$

$$(E_p)_i = \frac{1}{2}\varpi_i (Q_R - Q_o)_i^2 \tag{4}$$

$$(E_{vib})_i = (E_k)_i + (E_p)_i \tag{5}$$

where μ is the reduced mass and ϖ_i is the eigenvalue of mode, i. Next, assuming the harmonic approximation (independently of whether energy is computed using a harmonic, NMA-HARM, or anharmonic, NMA-ANHARM, approach) the action variable, n_i, is calculated from the vibrational energy and harmonic vibrational frequency using the well-known expression

$$(E_{vib})_i = (n_i + 1/2)\hbar\omega_i \tag{6}$$

and rounded to the nearest integer to obtain the vibrational quantum number of mode i.

It is well known that one of the difficulties with quasi-classical simulations is related to the question of how to handle the zero-point energy (ZPE) problem. Many strategies have been proposed to correct this QM effect,[29−48] but no really satisfactory alternatives have emerged. Here we employed a pragmatic solution, the so-called passive method, even knowing that this method perturbs the statistics and therefore can lead to uncertainties in the dynamics study.[49] We used two approaches. The first discards all reactive trajectories that lead to either the H_2 or the NH_2 product with a vibrational energy below their respective ZPEs. This we call histogram binning with double ZPE constraint, HB-DZPE. Schatz et al.[50,51] showed that in atom + triatom reactions this approach yields unphysically small cross sections, and they suggested that the ZPE constraint should be applied just to the newly formed bond. In the present case, it is applied only to the H_2 product. This we call histogram binning with ZPE-H_2 constraint, HB-ZPE-H_2.

The application of eq 1 requires the correct determination of the number of reactive trajectories, N_r, and the total number of trajectories, N_T, which are related to the ZPE problem, previously analyzed. So, we have three possible values of N_r: counting all reactive trajectories, only those that lead to both products with vibrational energy above their ZPE (HB-DZPE); and only those that lead to H_2 with vibrational energy above its ZPE (HB-ZPE-H_2). However, this way of removing trajectories from the N_r count without taking into account the behavior of the ensemble of trajectories can lend erroneous results because it modifies the statistics.[49] Recently, Bonnet[52] proposed an adiabaticity correction in atom + diatom reactions, which simply consists of omitting vibrationally adiabatic nonreactive trajectories in the calculations of final attributes. On the basis of these ideas and applied to polyatomic systems, here we count the total number of trajectories in two ways. First, as it has been usual in the QCT literature, we consider the total number of trajectories ran in the calculation, in our case, $N_T = 200\,000$. In the second approach, N_T in eq 1 is replaced by the total number of trajectories minus the number of reactive trajectories, whose final vibrational energy is below the ZPE of the two products or H_2 product (depending on whether we use the HB-

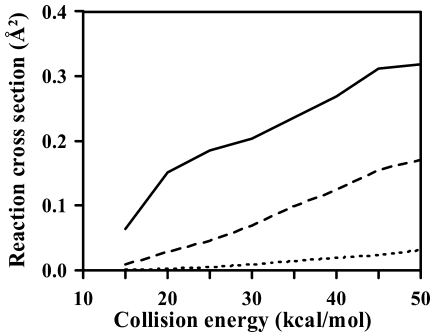

Figure 1. Excitation function (reaction cross section, in squared angstroms, versus the collision energy, in kilocalories per mole) computed using all reactive trajectories (solid line) and with the HB-ZPE-H_2 (dashed line) and HB-DZPE (dotted line) corrections. Energy range 15−50 kcal mol^{-1} in intervals of 5.0 kcal mol^{-1}.

DZPE or HB-ZPE-H_2 criterion), and minus the number of nonreactive trajectories whose final vibrational energy is below the ZPE of the NH_3 reactant. This number is called, N_T'. Therefore, we have six counting methods for the calculations of the reaction probability, (N_r/N_T), and therefore of the reaction cross section, eq 1: N_r^{all}/N_T, $N_r^{HB\text{-}DZPE}/N_T$, $N_r^{HB\text{-}ZPE\text{-}H2}/N_T$, N_r^{all}/N_T', $N_r^{HB\text{-}DZPE}/N_T'$, and $N_r^{HB\text{-}ZPE\text{-}H2}/N_T'$. These alternatives will be tested against QM calculations.

As mentioned above, the ZPE problem is an important issue in QCT calculations that still remains unsolved. In this respect, it is important to note that because of the numerical integration it must be expected that essentially every trajectory loses or gains some energy; that is, exact conservation of ZPE should not be expected even if there is no interaction between the reactants during a particular trajectory. Therefore, discarding all nonreactive trajectories with energy below the ZPE also could present uncertainties. For this reason, it is so important that the integration step be small enough to ensure conservation of the energy. Therefore, with the step-size used here, the vibrational energy was checked to be conserved with accuracy higher than 0.1 kcal/mol, which implies errors of <5% when computing N_r and N_T. In addition, because this error occurs both in the numerator and denominator of eq 1, some error cancellation can be expected. Therefore, one can safely assume that in our study and using a step size of 0.01 fs, numerical uncertainties due to the trajectory integration can be neglected.

III. Results and Discussion

A. Reaction Cross Section and Excitation Function. The excitation function (reaction cross section versus collision energy) is the only dynamics property theoretically analyzed for this reaction by other workers;[12−17] unfortunately, there are no experimental data for comparison. Figure 1 plots this function for the energy range 15−50 kcal mol^{-1} in intervals of 5.0 kcal mol^{-1} using the total number of trajectories, N_T. The reaction cross sections are small, even when the collision energy is 50 kcal mol^{-1}, and show a typical threshold behavior increasing with energy. These small values and this behavior agree with other theoretical studies[12−17] using different PESs and QCT or QM calculations but the same counting method, N_T. Moreover, these small values have been observed in other atom−polyatom reactions, such as the H + CD_4 reaction,[18] and this feature seems typical of polyatomic reactions with major steric effects, unlike atom−diatom reactions such as H + H_2.

Next, we analyze the influence of the counting method on this property. First, counting the total number of trajectories, N_T, we have tested the influence of the zero-point energy constraint on this property by performing calculations considering all trajectories and then removing the trajectories with energies below the ZPE of the products, HB-DZPE correction, and also removing the trajectories with energies below the ZPE in the newly formed H_2 product, HB-ZPE-H_2 (Figure 1). As was expected, the results were very sensitive to the ZPE criterion used. For instance, at 25 kcal mol^{-1}, the highest and lowest values are 0.185 and 0.005 $Å^2$ when all reactive trajectories are considered and when the very restrictive HB-DZPE correction is applied, respectively. In this latter case, the reaction cross section is excessively small. The HB-ZPE-H_2 correction presents an intermediate behavior with a value of 0.05 $Å^2$. As was noted above, there are no experimental data for comparison. Therefore, to validate the accuracy of these approaches, we used previous QCT and reduced dimensionality QM results[15] on a modified version of the PES-1997 surface. We shall use the QM results at a collision energy of 23.06 kcal mol^{-1} as a benchmark. Whereas the QM results predicted a very small cross section, 0.11 $Å^2$, the QCT calculations with all of the trajectories considered gave a value of 0.252 $Å^2$, notably overestimating the QM value. When the HB-DZPE constraint was applied, this value was drastically reduced to 0.003 $Å^2$. Finally, when the HB-ZPE-H_2 constraint was applied, a value of 0.056 $Å^2$ was obtained, which is about half the value of the QM result. Part of the differences between QCT and QM calculations can be explained by taking into account, first, that QCT calculations do not consider the tunneling effect, which is present in QM calculations, and second, the reduced dimensionality of the QM calculations. Therefore, the HB-ZPE-H_2 approach seems to work reasonably well in this reaction within the limitations of the classical QCT method, and the HB-DZPE correction seems to be an excessively strong constraint. Therefore, in the rest of article, we use the HB-ZPE-H_2 criterion for the dynamics analysis. Note that full-dimensionality QM calculations are being performed on the new PES-2009, and preliminary results confirm these results.

TABLE 1: Product Energy Partitioning (In Percentage) at Different Collision Energies[a]

collision energy	25	35	45
f_v (NH_2)	18 (19)[b]	15 (16)	13 (14)
f_r (NH_2)	3 (4)	3 (4)	4 (5)
f_v (H_2)	24 (11)	23 (13)	21 (13)
f_r (H_2)	9 (10)	9 (10)	11 (10)
f_t	46 (56)	50 (57)	51 (57)

[a] All energies are given in kilocalories per mole. [b] In parentheses are the results considering all reactive trajectories.

Second, we use the modified total number of trajectories, N_T'. Therefore, at 25 kcal mol^{-1}, the values are 0.336, 0.011, and 0.085 $Å^2$, respectively, when all reactive trajectories are considered, when the HB-DZPE correction is applied, and when the HB-ZPE-H_2 constraint is considered, which are about double the values of the counting considering N_T. The counting method, $N_r^{HB\text{-}ZPE\text{-}H2}/N_T'$, reproduces the QM results better, taking into account the fact that different PESs (although closely related) were used. This analysis illustrates the importance of avoiding criteria based on individual trajectories because QM constraints apply to ensembles.[49]

B. Product Energy Partitioning. The QCT product energy partitioning at different collision energies on the PES-2009 surface is listed in Table 1, where f_v, f_r, and f_t are the fractions of the available energy appearing in vibration, rotation, and translation, respectively, and the HB-ZPE-H_2 approach is used. Unfortunately, there are neither experimental nor theoretical data for comparison.

TABLE 2: Vibrational Populations (in Percentage) for the H_2 Product at Different Collision Energies

	E_c = 25 kcal mol^{-1}			E_c = 40 kcal mol^{-1}		
v	EBK	HARM	ANHARM	EBK	HARM	ANHARM
0	98	94	98	88	79	88
1	2	6	2	11	17	11
2				1	3	1
≥2					1	

First, the product energy partitioning is practically independent of the collision energy. Second, most of the available energy goes to translation (∼50%), followed by the internal energy of the H_2 product (∼30%) and the internal energy of the NH_2 product (∼20%). When all reactive trajectories are considered (values in parentheses in Table 1), that is, without removing trajectories with energies below the ZPE of the products, unsurprisingly, the internal energy of the H_2 product diminishes (∼23%), increasing the translational energy (∼57%). This is the expected result because now one is considering trajectories with a vibrational energy lower than the ZPE of H_2 and therefore with less energy going to vibrational motion. The results are thus again very sensitive to the chosen ZPE criterion.

These results agree with those for the H + HOD reaction,[50] in which 57−64% of the available energy goes to translation, or those for the H+CD_4 reaction,[53] in which 55−68% goes to translation. All of these reactions show a skew angle of 47°. Because this observable depends on the mass factor, these reactions, to some extent, present kinematics constraints.

C. $H_2(v',j')$ Product Rovibrational Distribution. The QCT populations of the vibrational levels of the diatomic H_2 product are listed in Table 2 using the EBK semiclassical approach and the NMA method (harmonic and anharmonic versions). Note that the HB-ZPE-H_2 binning histogram method is used.

At the lowest energy considered here, 25 kcal mol^{-1}, we find that the H_2 molecule is practically in its vibrational ground state. Because there is little vibrational excitation, the observed agreement between the NMA-anharmonic and EBK results is perfect. The NMA-harmonic results show more vibrational excitation, although the differences are small. At high energy, 40 kcal mol^{-1}, the vibrational excitation increases, and the differences between harmonic and anharmonic NMA also increase. However, our semiclassical NMA-anharmonic method reproduces the EBK values. These results at 25 and 40 kcal mol^{-1} agree with those obtained by Valentini et al.[18] for the isolectronic H + CD_4 → HD + CD_3 reaction at 34.6 kcal mol^{-1}. Those workers found that >95% of the HD product molecules are formed in the $v' = 0$ and 1 vibrational states.

The rovibrational state distributions of the H_2 product using the HB-ZPE-H_2 constraint, where the rotational number is truncated to the lowest integer value, are plotted in Figure 2 at two collision energies, 25 and 40 kcal mol^{-1}. One observes first that the rotational distribution is cold, peaking at $j' = 3$ at 25 kcal mol^{-1}, although there is a long tail; that is, the rotational distribution extends to high values of j', $j' = 10$. However, it is well known that the QCT calculations give rotational distributions hotter and broader than those of experiment and QM methods.[54−60] Let us consider this drawback of the QCT methods further. Therefore, using the harmonic approximation, the first excited vibrational state H_2 ($v' = 1$) is 12.6 kcal mol^{-1} ($\nu' =$ 4401 cm^{-1}) above the ground state. The QCT results show that the H_2 rotational population is non-negligible up to $j' = 10$. With a rotational constant $B = 60.85$ cm^{-1}, this implies an energy (assuming the rigid rotor model) of 19.1 kcal mol^{-1}, which is higher than the first vibrational state energy. In other words, the maximum value of j allowed in the vibrational ground state is $j' = 8$, that is, two units less than that obtained in the QCT calculations. This behavior therefore seems to be an artifact of the QCT methods, and recently our group[53] showed that it has important consequences in the scattering angle calculation. This effect will be analyzed below in Subsection E. Therefore, in a full quantum dynamics treatment, a colder and narrower rotational distribution could be expected.

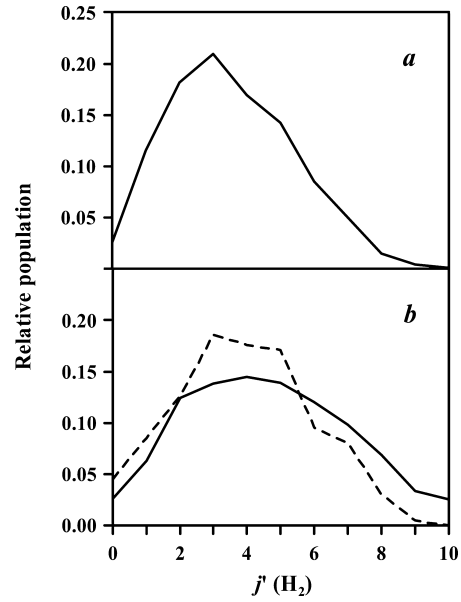

Figure 2. Rotational populations for H_2 (v',j') product computed using the HB-ZPE-H_2 histogram binning for the $v' = 0$ (solid line) and 1 (dashed line) vibrational states at a collision energy of (a) 25 and (b) 40 kcal·mol^{-1}.

Second, at 40 kcal mol^{-1}, where more H_2 vibrational states are populated, there is a normal negative correlation of product vibrational and rotational excitation; that is, when the vibrational state is excited, $v' = 1$, the rotational excitation is lower. Therefore, the rotational population peaks at $j' = 4$ and 3 for $v' = 0$ and 1, respectively. This result agrees with the universal behavior for direct bimolecular reactions.

D. $NH_2(v')$ Coproduct Vibrational Distribution. Figures 3 and 4 plot the QCT populations of the vibrational levels of the triatomic NH_2 species at two collision energies, 25 and 40 kcal mol^{-1}, respectively, using three approaches, FFT (panel a), NMA-HARM (panel b), and NMA-ANHARM (panel c), and where the HB-ZPE-H_2 method is used to treat the ZPE problem.

At 25 kcal mol^{-1}, the three methods used (Figure 3a−c) give practically the same picture. Almost 80% of the amidogen product is found in its vibrational ground state, ∼15% has one quantum of vibrational excitation in the bending mode, (0,1,0), and the rest populates various of the lowest excited vibrational states, (0,2,0), (1,0,0), and (0,0,1), at about 1 to 2%.

When the collision energy increases, 40 kcal mol^{-1} (Figure 4), the situation is practically the same; that is, the collision energy has little influence on the vibrational distribution in the NH_2 coproduct. Therefore, the population of the vibrational ground state, (0,0,0), diminishes slightly being populated at about 77%, while the bending mode with one quantum of vibrational excitation, (0,1,0), increases slightly, 17%, as well as the bending mode with two quanta, (0,2,0), 3%.

We tested the influence of the ZPE constraint on this property. When all reactive trajectories were considered, we obtained similar results and therefore do not plot them here. For instance,

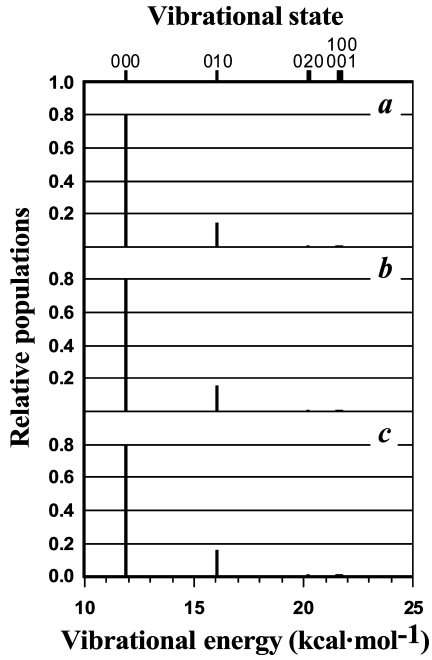

Figure 3. Relative populations of the vibrational states of the NH_2 product at a collision energy of 25 kcal mol^{-1} in the $H + NH_3 \rightarrow H_2 + NH_2$ reaction labeled (l, m, n), where l is the quantum number for the asymmetric stretching, m is the quantum number for the bending, and n is the quantum number for the symmetric stretching mode, as computed using the (a) FTT, (b) armonic NMA, and (c) anharmonic NMA methods.

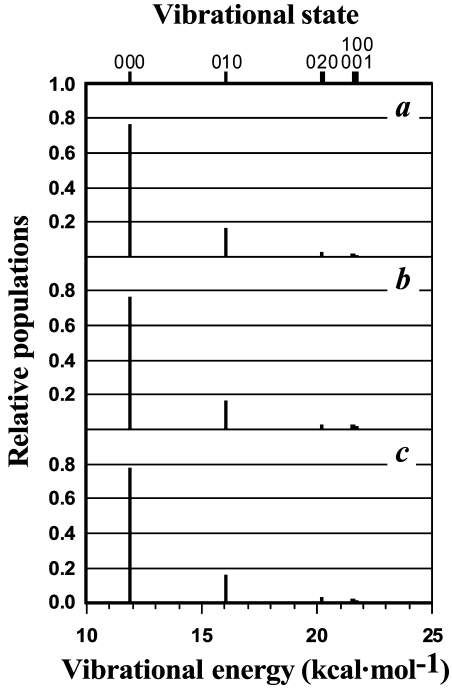

Figure 4. Same as Figure 3 but at a collision energy of 40 kcal·mol^{-1}.

for the NMA-HARM approach at 25 kcal mol^{-1}, the vibrational populations are 79 and 15% for the (0, 0, 0) and (0, 1, 0) states, respectively, versus 80 and 16% obtained when the HB-ZPE-H_2 constraint was applied.

The agreement between the three panels for the two collision energies, 25 and 40 kcal mol^{-1}, is excellent, showing first that anharmonicity is not important in this case and second that the distribution of the vibrational energy among modes is correctly described by the NMA method.[25]

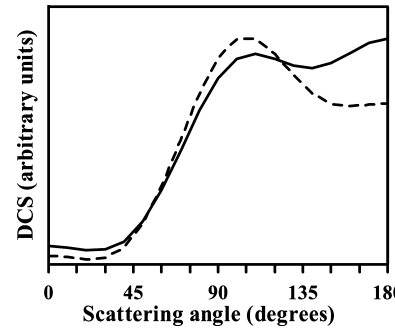

Figure 5. H_2 product angular distribution (with respect to the incident H) for the $H + NH_3 \rightarrow H_2 + NH_2$ reaction at 25 kcal·mol^{-1} computed using all reactive trajectories (solid line) and with the HB-ZPE-H_2 correction (dashed line).

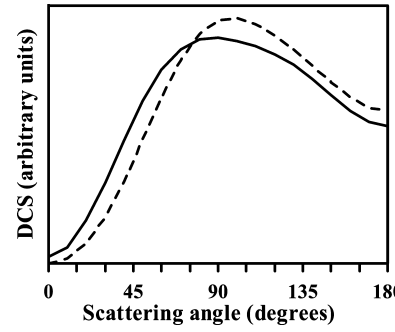

Figure 6. Same as Figure 5 but for a collision energy of 40 kcal·mol^{-1}.

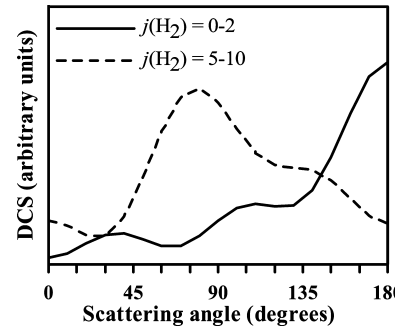

Figure 7. H_2 product angular distribution (with respect to the incident H) at 25 kcal·mol^{-1} on the PES-2009 surface as a function of the H_2 product rotational quantum number.

E. Differential Cross Section. The angular distributions of the H_2 product with respect to the incident H atom (obtained as the differential cross sections (DCSs), which are fitted by the Legendre moment method[61]) are plotted in Figures 5 and 6 for collision energies of 25 and 40 kcal mol^{-1}, respectively. At 25 kcal mol^{-1}, the scattering distribution is in the sideways−backward hemisphere. When all trajectories are considered, the backward contribution loses importance. When the collision energy increases, 40 kcal mol^{-1} (Figure 6), the scattering is shifted toward the sideways hemisphere, and at this energy, the ZPE constraint has no significant effect.

To shed more light on the QCT product angular distributions, we now analyze the QCT results for the H_2 (v',j') product as a function of j' (Figure 7) at 25 kcal mol^{-1}. It can be seen that for low values of j', $j' = 0-2$, the maximum of the DCS is located at ~180°, that is, practically backward. As j' is increased, the scattering is shifted toward the sideways hemisphere. As a result, when all j' values are included (Figure 5), the QCT scattering is predicted to be sideways−backward. However, as pointed out above, the contribution of high j' states seems to

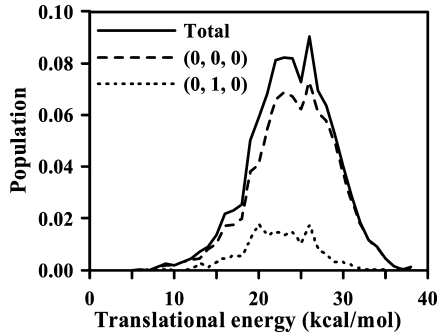

Figure 8. Product translational energy distribution (PTD) obtained with QCT calculations at a collision energy of 25 kcal·mol^{-1}.

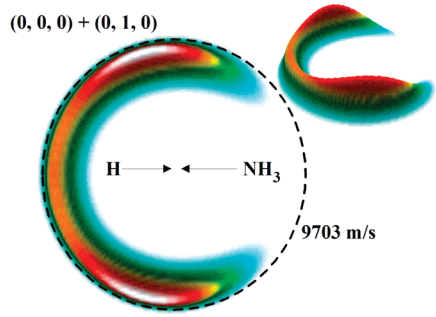

Figure 9. QCT polar scattering 3D surface plot and contour map of the CM scattering angle−velocity distribution, $P(\omega,\theta)$, for the H_2 products of the H + NH_3 → H_2 + NH_2 reaction at 25.0 kcal mol^{-1}. The maximum relative velocity of the coproducts is shown.

be an artifice of the QCT methods. Therefore, in a full quantum dynamical treatment, a more backward angular distribution could be expected, typical of a direct reaction with a rebound mechanism associated with low impact parameters.

The QCT product translational energy distributions at collision energy of 25 kcal mol^{-1} are plotted in Figure 8 for the (0, 0, 0) and (0, 1, 0) vibrational states and their sum. We found a broad peak with a maximum at ~23 kcal·mol^{-1}, which is the sum of the two vibrational states. The two states peak at similar energies and hence overlap so that only one peak will be detected experimentally.

The surface plots representing the doubly DCS, $d^2\sigma/[d\omega d\cos(\vartheta)]$, in center-of-mass polar coordinates (ω,θ) are shown in Figure 9 at a collision energy of 25 kcal mol^{-1}. All states show a sideways−backward scattering with the (0, 1, 0) state increasing the backward scattering.

IV. Conclusions

We have presented a detailed state-to-state dynamics study of the H + NH_3 hydrogen abstraction reaction using QCT calculations on a new analytical PES recently developed by our group, which is based exclusively on ab initio calculations.

The reactivity of the reaction, measured through the reaction cross section, is low in the collision energy range of 15−50 kcal mol^{-1}. Unfortunately, there are no experimental data for comparison, but this result agrees with other theoretical results on this reaction and with other atom−polyatom reactions, such as H + CD_4, showing the importance of steric effects and mainly the barrier height.

The vibrational distributions of the diatomic H_2 and triatomic NH_2 products were analyzed taking different approaches, including an anharmonic NMA approach recently developed in our group. The diatomic H_2 product is found to be vibrationally cold, $v' = 0,1$, with the vibrational excitation increasing with collision energy. The triatomic NH_2 product is found also to be vibrationally cold, with about 75−80%, depending on the collision energy, in its ground-state. The excellent agreement between our NMA and other more sophisticated methods for diatomic and triatomic species allows one to be optimistic about the application of this method to species with more than three atoms, for which other general methods are not available.

The product angular distribution appears in the sideways−backward hemisphere, indicating mainly a rebound mechanism associated with low impact parameters. When the collision energy increases, this distribution is shifted toward the sideways zone.

We found that the ZPE constraint affects the reaction cross section and the product energy partitioning, whereas the other dynamics properties that were analyzed (rovibrational distributions of the products and DCS) are practically independent of the ZPE problem.

Finally, we hope that the state-to-state dynamics study presented in this article for the H + NH_3 hydrogen abstraction reaction will stimulate future experiments.

Acknowledgment. This work was partially supported by the Junta de Extremadura, Spain (project no. PRI07A009).

References and Notes

(1) Dove, J. E.; Nip, W. S. *J. Chem. Phys.* **1974**, *52*, 1171.
(2) Michael, J. V.; Sutherland, J. W.; Klemm, R. B. *J. Phys.: Condens. Matter* **1985**, *17*, 315.
(3) Marshall, P.; Fontijn, A. *J. Chem. Phys.* **1986**, *85*, 2637.
(4) Sutherland, J. W.; Michael, J. V. *J. Chem. Phys.* **1988**, *88*, 830.
(5) Ko, T.; Marshall, P.; Fontijn, A. *J. Phys. Chem.* **1990**, *94*, 140.
(6) Friedrichs, G.; Wagner, H. G. *Z. Phys. Chem.* **2000**, *214*, 1151.
(7) Gordon, M. S.; Gano, D. R.; Boatz, J. A. *J. Am. Chem. Soc.* **1983**, *105*, 5771.
(8) Leroy, G.; Sana, M.; Tinant, A. *Can. J. Chem.* **1985**, *63*, 1447.
(9) Garrett, B. C.; Koszykowsky, M. L.; Melius, C. F.; Page, M. *J. Phys. Chem.* **1990**, *94*, 7096.
(10) Espinosa-Garcia, J.; Corchado, J. C. *J. Chem. Phys.* **1994**, *101*, 1333.
(11) Corchado, J. C.; Espinosa-Garcia, J. *J. Chem. Phys.* **1997**, *106*, 4013.
(12) Moyano, G. E.; Collins, M. A. *Theor. Chem. Acta* **2005**, *113*, 225.
(13) Li, H.; Liu, X.-G.; Zhang, Q.-G. *Chin. Phys. Lett.* **2005**, *22*, 1093.
(14) Zhang, X.-Q.; Cui, Q.; Zhang, J. Z. H.; Han, K. L. *J. Chem. Phys.* **2007**, *126*, 234304.
(15) Yang, M.; Corchado, J. C. *J. Chem. Phys.* **2007**, *126*, 214312.
(16) Yang, M.; Corchado, J. C. *J. Chem. Phys.* **2007**, *127*, 184308.
(17) Yang, M. *J. Chem. Phys.* **2008**, *129*, 064315.
(18) German, G.; Huh, T.; Valentini, J. *J. Chem. Phys.* **1992**, *96*, 1957.
(19) Camden, J. P.; Bechtel, H. A.; Zare, R. N. *Angew. Chem., Int. Ed.* **2003**, *42*, 5227.
(20) Espinosa-Garcia, J.; Corchado, J. C. *J. Phys. Chem. A* **2010**, *114*, 4455.
(21) Porter, R. N.; Raff, L. M. In *Dynamics of Molecular Collisions, part B*; Miller, W. H., Ed.; Plenum Press: New York, 1976.
(22) Truhlar, D. G.; Muckerman, J. T. In *Atom-Molecules Collision Theory*; Bernstein, R. B., Ed.; Plenum Press: New York, 1979.
(23) Raff. L. M.; Thompson, D. L. In *Theory of Chemical Reaction Dynamics*; Baer, M., Ed.; CRC Press: Boca Raton, FL, 1985; Vol. 3.
(24) Hase, W. L.; Duchovic, R. J.; Hu, X.; Komornicki, A.; Lim, K. F.; Lu, D.-h.; Peslherbe, G. H.; Swamy, K. N.; van de Linde, S. R.; Varandas, A. J. C.; Wang, H.; Wolf, R. J. *QCPE Bull.* **1996**, *16*, 43.
(25) Corchado, J. C.; Espinosa-Garcia, J. *Phys. Chem. Chem. Phys.* **2009**, *11*, 10157.
(26) Hase, W. L.; Duchovic, R. J.; Hu, X.; Komornicki, A.; Lim, K. F.; Lu, D.-h.; Peslherbe, G. H.; Swamy, K. N.; van de Linde, S. R.; Varandas, A. J. C.; Wang, H.; Wolf, R. J. *QCPE Bull.* **1996**, *16*, 671.
(27) Eaker, C. W.; Schatz, G. C. *J. Chem. Phys.* **1984**, *81*, 2394.
(28) Schatz, G. C. *Comput. Phys. Commun.* **1988**, *135*, 51.
(29) Wu, S. F.; Marcus, R. A. *J. Phys. Chem.* **1970**, *53*, 4026.
(30) Bowman, J. M.; Kuppermann, A. *J. Chem. Phys.* **1973**, *59*, 6524.
(31) Truhlar, D. G. *J. Phys. Chem.* **1979**, *83*, 18.
(32) Schatz, G. C. *J. Chem. Phys.* **1983**, *79*, 5386.
(33) Lu, D.-h.; Hase, W. L. *J. Chem. Phys.* **1988**, *89*, 6723.
(34) Nyman, G.; Davidsson, J. *J. Chem. Phys.* **1990**, *92*, 2415.
(35) Wilhelmsson, U.; Nyman, G. *J. Chem. Phys.* **1992**, *96*, 1886.

(36) Varandas, A. J. C.; Brandão, J.; Pastrana, M. R. *J. Chem. Phys.* **1992**, *96*, 5137.
(37) Varandas, A. J. C.; Marques, J. M. C. *J. Chem. Phys.* **1994**, *100*, 1908.
(38) Varandas, A. J. C. *Chem. Phys. Lett.* **1994**, *225*, 18.
(39) Ben-Nun, M.; Levine, R. D. *J. Chem. Phys.* **1994**, *101*, 8768.
(40) Wang, X.; Ben-Nun, M.; Levine, R. D. *Chem. Phys.* **1995**, *197*, 1.
(41) Ben-Nun, M.; Levine, R. D. *J. Chem. Phys.* **1996**, *105*, 8136.
(42) Bonnet, L.; Rayez, J. C. *Chem. Phys. Lett.* **1997**, *277*, 183.
(43) McCormack, D. A.; Lim, K. F. *Phys. Chem. Chem. Phys.* **1999**, *1*, 1.
(44) Stock, G.; Müller, U. *J. Chem. Phys.* **1999**, *111*, 65.
(45) Müller, U.; Stock, G. *J. Chem. Phys.* **1999**, *111*, 77.
(46) Bonnet, L.; Rayez, J. C. *Chem. Phys. Lett.* **2004**, *397*, 106.
(47) Marques, J. M. C.; Martinez-Nuñez, E.; Fernandez-Ramos, A.; Vazquez, S. *J. Phys. Chem.* **2005**, *109*, 5415.
(48) Duchovic, R. J.; Parker, M. A. *J. Phys. Chem.* **2005**, *109*, 5883.
(49) Guo, Y.; Thomson, D. L.; Sewell, T. D. *J. Chem. Phys.* **1996**, *104*, 576.
(50) Kudla, K.; Schatz, G. C. *Chem. Phys.* **1993**, *175*, 71.
(51) Bethardy, G. A.; Wagner, A. F.; Schatz, G. C.; ter Horst, M. A. *J. Chem. Phys.* **1997**, *106*, 6001.
(52) Bonnet, L. *J. Chem. Phys.* **2008**, *128*, 044109.
(53) Espinosa-Garcia, J.; Nyman, G.; Corchado, J. C. *J. Chem. Phys.* **2009**, *130*, 184315.
(54) Bañares, L.; Aoiz, F. J.; Honvault, P.; Bussery-Honvault, B.; Launay, J.-M. *J. Chem. Phys.* **2003**, *118*, 565.
(55) Gerrity, D. P.; Valentini, J. J. *J. Chem. Phys.* **1984**, *81*, 1298.
(56) Kliner, D. A. V.; Rinnen, K. D.; Zare, R. N. *Chem. Phys. Lett.* **1990**, *166*, 107.
(57) Bean, B. D.; Fernandez-Alonso, F.; Zare, R. N. *J. Phys. Chem. A* **2001**, *105*, 2228.
(58) Bean, B. D.; Ayers, J. D.; Fernandez-Alonso, F.; Zare, R. N. *J. Chem. Phys.* **2002**, *116*, 6634.
(59) Pomerantz, A. E.; Ausfelder, F.; Zare, R. N.; Althorpe, S. C.; Aoiz, F. J.; Bañares, L.; Castillo, F. J. *J. Chem. Phys.* **2004**, *120*, 3244.
(60) Xie, T.; Bowman, J. M.; Duff, J. W.; Braunstein, M.; Ramachandran, B. *J. Chem. Phys.* **2005**, *122*, 014301.
(61) Truhlar, D. G.; Blais, N. C. *J. Chem. Phys.* **1977**, *67*, 1532.

JP101607N